Space based observation of volcanic iodine monoxide

Anja Schönhardt[1], Andreas Richter[1], Nicolas Theys[2], and John P. Burrows[1]

[1]Institute of Environmental Physics, University of Bremen, Otto-Hahn-Allee 1, 28359 Bremen, Germany.
[2]Belgian Institute for Space Aeronomy, Avenue Circulaire 3, B-1180 Brussels, Belgium.

Correspondence to: Anja Schönhardt (schoenhardt@iup.physik.uni-bremen.de)

Abstract.

Volcanic eruptions inject substantial amounts of halogens into the atmosphere. Chlorine and bromine oxides have frequently been observed in volcanic plumes from different instrumental platforms, from ground, aircraft as well as from satellite. The present study is the first observational evidence that iodine oxides are also emitted into the atmosphere during volcanic eruptions. Large column amounts of iodine monoxide, IO, have been observed in satellite measurements following the major eruption of the Kasatochi volcano, Alaska, in 2008. The IO signal is detected in measurements made both by SCIAMACHY on ENVISAT and GOME-2 on MetOp-A. Following the eruption on August 07, 2008, strongly elevated levels of IO slant columns of more than 4×10^{13} molec/cm^2 are retrieved along the volcanic plume trajectories for several days. The retrieved IO columns from the different instruments are consistent and the spatial distribution of the IO plume is similar to that of BrO. Details in the spatial distribution, however, differ between IO, BrO and sulphur dioxide, SO$_2$. The columns of IO are approximately one order of magnitude smaller than those of BrO. Using the GOME-2A observations, the total mass of IO in the volcanic plume injected into the atmosphere from the eruption of Kasatochi on August 07, 2008, is determined to be on the order of 10 Mg.

1 Introduction

Halogen oxides strongly influence atmospheric composition. Catalytic reaction cycles involving chlorine, bromine or iodine, lead to ozone depletion in the troposphere. In the stratosphere, the role of chlorine and bromine released predominantly as a consequence of anthropogenic emissions of chlorofluorocarbon compounds is well established (World Meteorological Organization, 2014), and the potential importance of iodine reactions in stratospheric ozone depletion is discussed (Solomon et al., 1994; Saiz-Lopez et al., 2015a). Stratospheric concentrations of iodine species are much lower than those of chlorine and bromine (Bösch et al., 2003). However, the ozone destruction potential of stratospheric iodine is significantly higher than that of the other halogens. The destruction of ozone is about 60 times more effective for bromine and about 150-300 times more effective for iodine as compared to chlorine (World Meteorological Organization, 2014). The effective chain length of the catalytic cycles involving iodine and iodine monoxide, IO, is larger than those involving the other halogens. This is in part because the temporary reservoir species containing iodine are photolysed and/or react more rapidly with stratospheric free radicals than their chlorine or bromine analogies. Recent measurements and modeling studies conclude that iodine injection into the stratosphere is currently underestimated (Saiz-Lopez et al., 2015a), and that stratospheric amounts of reactive iodine

lie between 0.25-0.7 parts per trillion by volume (pptv). Even at sub-pptv levels, reactive iodine may significantly impact on stratospheric ozone chemistry.

IO is formed from the reaction of iodine radicals with ozone, O_3. Catalytic cycles including IO were proposed already in the 1980s by which tropospheric O_3 is effectively destroyed (Chameides and Davis, 1980). As a result of self-reactions, iodine

5 oxides may lead to particle formation and thereby affect atmospheric radiation balance (Burkholder et al., 2004; O'Dowd and Hoffmann, 2005; Saunders et al., 2010). These issues motivate the scientific interest in the assessment of sources, amounts and distributions of iodine species in the atmosphere.

Atmospheric iodine is of organic as well as inorganic origin, e.g., from emissions of I_2 and of halogenated organic compounds such as CH_3I and CH_2I_2 (Saiz-Lopez et al., 2012, and references therein). The largest iodine source in general are the world's

10 oceans. Iodine compounds have been shown to be emitted into the marine boundary layer, e.g., from algae (Schall et al., 1994; Alicke et al., 1999; Carpenter, 2003) or via inorganic pathways involving the ocean surface (Garland and Curtis, 1981; Carpenter et al., 2013). In the Polar troposphere, both, bromine and iodine oxides, are observed predominantly during spring time. Release mechanisms of iodine and bromine above sea ice areas, however, are considerably different. Bromine monoxide, BrO, is released following an autocatalytic Br activation (Vogt et al., 1999), also known as the bromine explosion mechanism.

15 Iodine most probably takes different pathways involving the release of organo-iodine compounds (Saiz-Lopez et al., 2015b), but inorganic reactions cannot be excluded.

Volcanic eruptions are an important source of halogens in the atmosphere, especially for the free and upper troposphere and the lower stratosphere (von Glasow et al., 2009). Volcanic plumes are known to contain halogen species, initially in acidic form, e.g., HF, HCl, HBr and HI (Aiuppa et al., 2009). Bromine oxides as well as chlorine oxides have been previously observed

20 in volcanic plumes. Volcanic BrO was first observed by Bobrowski et al. (2003) who applied the well established Differential Optical Absorption Spectroscopy (DOAS) technique (Platt and Stutz, 2008) with a ground-based Multiple AXis DOAS (MAX-DOAS) system. Volcanic chlorine oxides, ClO and OClO, were measured e.g. by Lee et al. (2005) and Bobrowski et al. (2007), also using ground-based DOAS instruments. From space, volcanic BrO was detected for the first time from the Kasatochi eruption in 2008 (Theys et al., 2009), followed by volcanic OClO from the Puyehue eruption in 2011 (Theys et al.,

25 2014). Several further observations using ground-based measurements (Bobrowski et al., 2006; Bobrowski and Platt, 2007; Kern et al., 2009), airborne instrumentation (General et al., 2015) as well as satellites (Hörmann et al., 2013) have confirmed and further quantified the abundance of bromine oxides injected into the atmosphere following volcanic eruptions. The release mechanism of volcanic BrO is believed to be similar as for polar tropospheric BrO and is based on an autocatalytic reaction cycle involving volcanic aerosols (Bobrowski et al., 2007). Ozone depletion has been observed within volcanic plumes and is

30 attributed to reactive halogen chemistry (Lee et al., 2005; Surl et al., 2015, and references therein).

Using filter techniques, measurements at Mt. Etna in Italy (Aiuppa et al., 2005) and at Masaya and Telica volcanos in Nicaragua (Witt et al., 2008), for example, showed that gaseous HI, I and HBr are relevant constituents in the degassing of these specific volcanos. Only a few studies are available that report on samples of volcanic gases or volcanic fluids, which have been analysed for their iodine content. Snyder and Fehn (2002) investigate the $^{129}I/I$ ratio in volcanic fluids in order to determine the

35 ages of iodine species. The determined iodine ages are in agreement with the expected age of subducted sediments. An iodine

accumulation takes place, as marine sediments contain concentrated amounts of organic iodine.

The composition of volcanic gases is in general strongly variable with individual characteristics changing from volcano to volcano as well as between eruption and degassing phases (Witt et al., 2008; Aiuppa et al., 2009, and references therein). Although the gas phase composition is individual for each volcanic eruption, there is a general difference between iodine and other halogens in volcanic gases at high temperatures. Around $1000°$ C, the main constituents are HF, HCl, and HBr for the other halogens. For iodine, however, HI and atomic I may be present in equal amounts (Aiuppa et al., 2005).

Up to the present, no detection of gaseous iodine oxides of volcanic origin has been reported, neither by in-situ measurements nor by remote sensing from ground or satellite. Iodine monoxide has been retrieved from satellite measurements of backscattered solar radiation by the DOAS technique and has previously been observed from space, e.g., in the South Polar Region (Saiz-Lopez et al., 2007; Schönhardt et al., 2008, 2012). In most cases, atmospheric amounts of IO are fairly small, so that usually temporal averages of the satellite data of at least one month are created in order to improve signal-to-noise ratio.

In August 2008, the eruption of Kasatochi volcano took place (Waythomas et al., 2010). Kasatochi belongs to the volcanic arc of the Aleutan Islands, Alaska. The violent explosions started on August 07, 2008, in the afternoon. The Volcanic Explosivity Index (VEI) (Newhall and Self, 1982), which classifies the eruptive volume and eruption cloud height, was VEI 3-4. Large amounts of ash and sulphur dioxide, SO_2, were released to the atmosphere reaching the lower stratosphere (Waythomas et al., 2010). In total about 1.7 Tg SO_2 was emitted and spread over large parts of the globe.

In the following, the detection of IO from the eruption of Kasatochi volcano using observations of the SCIAMACHY and GOME-2A satellite instruments is presented and discussed. The applied instruments and retrieval settings are briefly described, and the IO spectral fit quality is investigated. The IO results are analysed in terms of spatial distribution, temporal evolution and integral amount. In addition, IO and BrO distributions in the volcanic plume are compared among each other and to those of sulphur dioxide, SO_2.

2 Instruments and Measurements

The only satellite borne spectrometer for which an IO product has been reported so far is the SCIAMACHY instrument (SCanning Imaging Absorption spectroMeter for Atmospheric CHartography) onboard the European Environmental Satellite (ENVISAT) (Saiz-Lopez et al., 2007; Schönhardt et al., 2008, 2012). The mission operated between March 2002 and April 2012. In this study, data from the GOME-2A (Global Ozone Monitoring Experiment) onboard MetOp-A (Meteorological Operational Satellite A) has also been successfully analysed and the signature of IO and BrO absorption has been retrieved. The IO detection from GOME-2A is reported here for the first time. The DOAS method has been used for the retrieval of trace gas amounts.

2.1 Satellite instruments and data

SCIAMACHY is a spectrometer measuring direct, scattered and reflected sun light in the UV, vis and near-IR spectral regions. The spectra are measured contiguously from 214 to 1773 nm and in two spectral bands within the ranges of 1934-2044 nm

and 2259-2386 nm. The operation modes include nadir, limb and occultation geometries (Burrows et al., 1995; Bovensmann et al., 1999; Gottwald, 2011). The present study uses the nadir observations. ENVISAT has a sun-synchronous, near-polar orbit with a local equator crossing time of 10:00 a.m. in descending node. Individual SCIAMACHY ground pixels in the spectral range used here have a typical size of $30 \times 60 \, \text{km}^2$. For the IO retrieval in general, spatial averaging over four ground pixels is

5 applied to reduce noise. A further reduction in spatial resolution occurs for some parts of each orbit as a result of using the SCIAMACHY read out from cluster 14 in channel 3 (404 - 424 nm) in addition to the more commonly used cluster 15 (424 - 527 nm). Cluster 14 has partly longer integration time than cluster 15, and the integration time is adapted for the entire spectral region to achieve smoothed spectra across the cluster border. Maximum across track ground scene pixel size is 240 km.

The GOME-2A instrument observes in the UV and visible spectral regions from 240 to 790 nm and performs measurements in

10 nadir viewing geometry. Launched in July 2006 onboard MetOp-A, GOME-2A is the first of three effectively nearly identical instruments. The mission officially started in October 2006 and data is available since 2007. The equator crossing time of MetOp-A is 09:30 a.m. As for SCIAMACHY, spatial averaging is applied for the GOME-2A data in order to achieve noise reduction. The typical ground pixel size of $40 \times 80 \, \text{km}^2$ is thus increased to $80 \times 160 \, \text{km}^2$. For some direct comparisons with BrO, however, the IO results without spatial averaging are used.

15 ## 2.2 DOAS retrievals of IO and BrO

The DOAS method is applied to the satellite measurements in order to retrieve IO and BrO column amounts. For the SCIA-MACHY IO product, the standard retrieval settings as published in Schönhardt et al. (2008) and summarized in Tab. 1 are used. Two example fitting results from day August 11, 2008, are displayed in Fig. 1 showing the spectral fits for IO columns of $4.9 \times 10^{13} \, \text{molec/cm}^2$ (top) and $2.3 \times 10^{13} \, \text{molec/cm}^2$ (bottom). The comparably large IO columns are connected to rather

20 small relative fitting errors of 5.3 and 8.3 %, respectively.

For the analysis of GOME-2A data, two alternative retrievals are used and also listed in Tab. 1. The 2T retrieval corresponds to the standard SCIAMACHY IO retrieval and therefore covers the same two IO transition bands. The GOME-2A data show higher noise levels than the respective SCIAMACHY measurements. Consequently, for the analysis of GOME-2A data, the use of more spectral information from a larger fitting window was investigated. The resulting 3T retrieval covers three tran-

25 sition bands of the IO absorption spectrum. For SCIAMACHY, the 3T retrieval had not been successful (Schönhardt et al., 2008) due to instrument related spectral features above 430 nm. It leads, however, to an improved quality of the IO retrievals from GOME-2A measurements. If not specified elsewise, GOME-2A IO results from the 3T retrieval are used. In terms of IO amounts the results are consistent within the uncertainties between both GOME-2A retrievals, as well as between GOME-2A and SCIAMACHY, cf. Sec. 3.2.

30 For all IO retrievals, a daily averaged Earthshine spectrum was used as reference background. This background spectrum was generated from a reference area $60°$ to $70°$ North and $80°$ to $120°$ East, a continental region which is assumed to have small column amounts of IO. So a differential slant column between the specific location and this reference region is retrieved.

The cross sections used for SCIAMACHY retrievals are $NO_2(223 \, \text{K})$ (Bogumil et al., 2003) and $O_3(223 \, \text{K})$ (Bogumil et al., 2003). For GOME-2A retrievals, $NO_2(223 \, \text{K})$ and $O_3(223 \, \text{K})$ from measurements with the GOME-2 flight model are used

Retrieval settings	SCIAMACHY	GOME-2A 2T	GOME-2A 3T
Fitting window	416-430 nm	416-430 nm	418-438 nm
Polynomial degree	2 (quadratic)	2 (quadratic)	3 (cubic)
Trace gases	NO_2, O_3	NO_2, O_3	NO_2, O_3, O_4
	IO	IO	IO
Other features	Ring effect: SCIATRAN calculation (Rozanov et al., 2014; Vountas et al., 1998)		
	Linear intensity offset correction		
Background	Daily Earthshine, Siberia (60°- 70°N, 80°-120°E)		

Table 1. Retrieval settings for IO from SCIAMACHY and GOME-2A observations.

(Chehade et al., 2013, and P. Spietz, private communication, 2005), as well as O_4 (Greenblatt et al., 1990) in addition for the GOME-2A 3T retrieval. For all retrievals the IO(298 K) cross section measured by Gómez Martín et al. (2007) is applied, convolved with the slit function of the respective instrument.

BrO columns are retrieved from GOME-2A in a fitting window from 336 to 347 nm taking into account absorption features of

5   O_3 (223 K and 273 K), NO_2 (223 K), and BrO (Begoin et al., 2010). A cubic polynomial with four coefficients is fitted for the broadband spectral effects.

SCIATRAN calculations (Rozanov et al., 2014) are used to determine reference spectra for rotational Raman scattering (Ring effect), which is taken into account in all retrievals. An additional additive intensity offset compensates for stray light, remaining Ring structures, or the influence of vibrational Raman scattering.

10   The DOAS analysis yields the trace gas slant column values, which are the absorber concentrations integrated along the mean light path. In order to convert these numbers into vertical column values, the air mass factor (AMF), i.e. the ratio between the slant and vertical column, is computed. For both, IO and BrO, a geometric AMF is applied here which is suitable for a stratospheric absorber. This is an adequate assumption for the current study as the volcanic plume is located at fairly high altitudes (Theys et al., 2009) and the relevant SZA values are below 50°. The influence of aerosols on light scattering and

15   thus on the AMF are not considered in this work. Aerosols can increase or decrease visibility of trace gases depending on several aspects such as aerosol characteristics and the relative altitude distributions. Here we concentrate on a more qualitative discussion of the observed halogen amounts.

3   Results

3.1   Observation of volcanic IO

20   Following the eruption of Kasatochi, enhanced IO amounts are visible for several days. As a consequence of the morning overpass times of the satellite instruments, the eruption which started in the afternoon of August 07, 2008, can be observed

from August 08, 2008, onwards. For six days from August 08 to August 13, the observational results from the SCIAMACHY IO retrieval are shown in Fig. 2, left column. IO enhancements are detected on all six days, as well as enhancements of BrO (not shown, see http://www.iup.uni-bremen.de/doas/scia_data_browser.htm?gas=bro&column=strat&view=nh&year=2008&month=8&day=8). On August 08, a loop shaped area with enhanced IO is visible, maximum slant column amounts being

5   around 2.3×10^{13} molec/cm^2. In the same area, BrO reaches slant column values up to 4.2×10^{14} molec/cm^2. The slant column amounts on August 09 are higher with 3.4×10^{13} molec/cm^2 and 5.6×10^{14} molec/cm^2 for IO and BrO, respectively. While on day August 10, the volcanic plume is situated just in between two SCIAMACHY orbits, and only slightly enhanced amounts are seen at the edges of the plume in the adjacent orbits (at 50°N, 210°E, and 55°N, 225°E), the SCIAMACHY IO amounts are largest on day August 11. Slant columns reach up to 4.9×10^{13} molec/cm^2 for IO and 5.6×10^{14} molec/cm^2 for BrO. These

10 values correspond to vertical columns of 2.1×10^{13} molec/cm^2 for IO and 2.5×10^{14} molec/cm^2 for BrO. While these large amounts of BrO from volcanic emission have been reported before (Theys et al., 2009), IO produced from volcanic activity is observed for the first time.

3.2   IO detection with GOME-2A

Maps of IO retrieved from GOME-2A data for the six days after the eruption are shown in Fig. 2 (middle) next to the SCIA-

15 MACHY results for direct comparison. BrO amounts retrieved from GOME-2A are shown in the right column. Due to the much better spatial coverage of the GOME-2A instrument, the IO plume from the volcanic emission is clearly visible on all six days. The spatial shape of the IO enhancement agrees well with the area where higher BrO is observed.

As a comparison of the IO results retrieved from the two different sensors, an example collocation case from August 11 has been chosen. The results including both GOME-2A retrievals as discussed in Sec. 2.2 are summarized in Tab. 2 and the corre-

20 sponding spectral fits are shown in Fig. 3.

The IO results of the three retrievals are consistent within their uncertainties. GOME-2A results also show good retrieval quality with a relative retrieval error of around 14 %, which is somewhat larger than for the SCIAMACHY examples. The IO detection limit for GOME-2A observations is on the order of 5×10^{12} molec/cm^2 in terms of vertical columns, and around 1×10^{13} molec/cm^2 for the retrieved slant columns, depending on several factors such as light intensity and solar zenith angle.

25 For the example case, GOME-2A detects slightly less IO than SCIAMACHY, however, in other collocation cases the relation is reverse. The ground scenes of the two instruments are not identical and the measurement times differ by typically half an hour. For a rapidly moving volcanic plume, in which relatively fast and complex multiphase photochemical reactions take place, some real differences in the IO amounts as seen by the two instruments are therefore expected.

3.3   Analysis of IO and BrO amounts

30 The sampling of GOME-2A measurements is intrinsically higher than that of SCIAMACHY and the full volcanic plume is observed on several days. Consequently, IO retrieved from GOME-2 yields a more accurate analysis of the total iodine amount and mass emitted from the Kasatochi eruption. Integration over the IO amount inside the plume is performed. For this purpose, first the plume itself needs to be defined. Here, it is determined as the area enclosing those satellite pixels with an IO amount

Retrieval results	SCIAMACHY	GOME-2A 2T	GOME-2A 3T
window	416-430 nm	416-430 nm	418-438 nm
SC_{IO} / 10^{13} molec/cm^2	4.58 ± 0.28	4.25 ± 0.60	4.14 ± 0.59

Table 2. IO retrieval results from the collocation case between SCIAMACHY and GOME-2A on 11.08.2008. The three results agree within their fitting errors.

above a certain threshold. This threshold $VC_{IO,thr}$ is defined as $VC_{IO,thr} = \langle VC_{IO} \rangle + 2\sigma_{IO}$, where $\langle VC_{IO} \rangle$ is the mean IO vertical column and σ_{IO} is the standard deviation, both derived from measurements on the days before the eruption as explained below. For BrO, the procedure is almost the same, but the threshold is set at $3\sigma_{BrO}$ above the mean. For IO, the weaker criterion of 2σ is necessary in order to capture the plume well. The reason for this is the larger noise as compared to that for

5 the BrO data, i.e. enhanced IO amounts are closer to the detection limit than is the case for BrO. Mean and standard deviation values for IO and BrO are calculated using the data from three days with satellite overpasses before the eruption (August 05 to 07, 2008) and from within a wide area around the volcano (40-62.5°N, 183.5-231°E) enclosing all main plumes on the consecutive days. Threshold values are 5.3×10^{12} molec/cm^2 and 9.7×10^{13} molec/cm^2 for IO and BrO, respectively. Only a small background IO slant column is found prior to the eruption (around 0.4×10^{12} molec/cm^2 and below the detection limit),

10 while the BrO column has a substantial stratospheric as well as free-tropospheric contribution of around 6.1×10^{13} molec/cm^2 in this area.

In an alternative approach, the observed SO$_2$ amount (cf. Sec 3.4) is used in order to select the BrO and IO in the volcanic plume. For this SO$_2$ mask approach, the plume is defined by applying a 10 DU limit to the SO$_2$ distribution. Following the plume definition and background subtraction, the IO and BrO amounts are integrated over the selected plume area yielding

15 an integrated number of molecules originating from the volcanic eruption. For the days August 08 to 12, the results of this procedure are shown as a timeseries for IO and BrO in Fig. 4. Results from the threshold criterion are displayed and compared with those obtained using the SO$_2$ mask approach.

On days August 08 to 11, the two methods agree within a few %, while the actual plume shape differs slightly at the edges. On August 12 the difference of the plume positions between SO$_2$ on one hand and BrO and IO on the other is larger. For

20 IO, the difference does not affect the integrated value much while for BrO the results from the two different selection routines differ by 60%. Using the SO$_2$ mask, part of the BrO plume is missed. For IO, values in that region were lower so the effect is less pronounced. In general, the two methods are in agreement, but due to the latter observation, the method using the σ-level criterion is preferred.

On day August 08 just after the start of the eruption, approximately 1.8×10^{28} molecules of IO are observed in the plume,

25 corresponding to a mass of 4.3 Mg or metric tons, t, of IO. The amount of IO increases to 7.7 t on August 09, reaches up to 12.2 and 12.1 t (i.e. around 5.1×10^{28} molecules of IO) on the peak days on August 10 and 11, respectively, and decreases back to 7.4 t on August 12. The range of IO values between 4.3 and 12.1 t corresponds to an amount of reactive iodine between 3.9

and 10.8 t.

The integrated amount of BrO within the plume increases from 26 t on August 08 to 76 t and 79 t on August 09 and 10, and reaches a maximum amount of 87 t on August 11. On August 12 an amount of 66 t of BrO remains. Converting this range of values between 26 and 87 t to the corresponding amount of reactive Br, amounts between 22 and 73 t are derived. These

5 integrated BrO amounts are larger but in broad agreement with calculations by Theys et al. (2009), who use the FLEXPART dispersion model and derive the total amount of BrO within the volcanic plume to be around 30 to 42 t. In addition to BrO, other bromine compounds contribute to the total bromine mass. In the relevant altitude between 8 and 12 km, 30-50% of the total inorganic bromine exist in the form of BrO (Theys et al., 2009). Using this relation, the integrated BrO amount corresponds to 50 to 290 t total mass of reactive bromine.

Although knowledge on iodine chemistry in a volcanic plume is limited, other iodine compounds such as I_2, I, HI , HOI, OIO and higher iodine oxides are presumably present in the emission plume as well. Consequently, the amount of iodine between 3.9 to 10.8 t derived here from the IO alone needs to be considered as a lower limit. The amount of iodine derived from the Kasatochi eruption is of the same order of magnitude determined by measurements at degassing volcanos for one

15 year, e.g. 10 t/yr of iodine at Mt. Etna, Italy, (Aiuppa et al., 2005) or 12 t/yr at Satsuma-Iwojima, Japan (Snyder and Fehn, 2002). This is in line with observations for bromine, where for one given volcano the Br flux from an individual eruption can be of the same order of magnitude as the annual Br flux from degassing (Aiuppa et al., 2005). The temporal evolution of the integrated amounts is discussed in Sec. 4.

3.4   Spatial distributions of IO, BrO and SO_2

20 In order to investigate the spatial plume structure more closely, Fig. 5 gives an expanded view of the volcanic plume. The retrieved amounts of IO (left) and BrO (center) are shown together with those of SO_2 (right) for the days August 09 (top) and August 11 (bottom). SO_2 amounts are derived in the spectral window between 312.5 and 327 nm using an iterative retrieval approach (Richter, 2009).

Previous satellite studies have observed that BrO is enhanced around the plume center (Hörmann et al., 2013). For the two

25 depicted cases, the IO amount is also lower in the plume center. In general, the IO and BrO plumes have similar spatial extent and shape. It is however interesting to note, that maximum IO and BrO amounts are not observed in the same satellite pixels, and that the details of the spatial patterns differ. On August 09, largest BrO enhancements are detected in the West and East of the plume, while IO is also enhanced there but even more in the South of the plume. On August 11, BrO maxima are seen in the West, and IO maxima are split into two regions in the North and South of the volcanic plume.

30 The IO and BrO data from within a rectangular latitude-longitude box enclosing the entire volcanic plume has been investigated individually for each day between August 08 and 12. The correlation coefficient between IO and BrO considering the data from the respective area lies between $R = 0.62$ and $R = 0.84$ on the days from August 09 to 12. On the first day, August 08, the correlation is lower at $R = 0.42$. These results with relatively large and positive values of R indicate that iodine and bromine compounds are emitted together into the volcanic plume, but also that there are factors influencing the temporal evolution

of the two gases differently as $R < 0.85$. The chemical pathways of iodine and bromine within the plume are probably not independent from each other. Formation and loss processes may interfere with each other. Although the rate coefficients for the reactions of I and Br with O_3 are similar, the smaller expected concentrations of I than Br imply that the time constant for IO production is slower than that for BrO. As a consequence, large amounts of Br that react with O_3, thereby strongly reducing

5 the O_3 abundance, may prevent the build-up of IO resulting in spatially separated maximum values for the two halogen oxides. The reactions between IO and BrO, as well as self reactions of IO impact on the spatial distributions and maximum amounts. Furthermore, the time of emission of the precursor substances may differ to some degree. Iodine and bromine have different solubility in volcanic fluids (Aiuppa et al., 2009). As a consequence, degassing from the magma may take place at different pressure, i.e. at different depth and time, for the two halogen species.

10 The IO and BrO distributions are again similar to those of SO_2, but even larger differences occur than between the distributions of the two halogen compounds. For SO_2, no occurrence of lower values in the plume center is observed. On some days, such as the example day August 11, SO_2 is at maximum in the plume center. On day August 09, two SO_2 maxima are seen, one part is crossing the plume center, and one part is situated more to the Southern edge of the plume. In general, the comparison between the trace gas spatial distributions is interesting because it yields potentially information on the eruption process and

15 chronology. Details of the plume composition and evolution need to be analysed in the future by chemical transport modeling to provide better insight into the complex reactions taking place within the plume.

4   Discussion

Comparing the integrated numbers of IO and BrO molecules in the volcanic plume, one important and interesting point is that the amount of iodine is only about one order of magnitude smaller than that of bromine. For the individual days August 09 to

20 12, the ratio for the integrated number of BrO to IO molecules lies between 6.7 and 10.0 (4.2 on August 08). The corresponding ratio for the mass of BrO to IO lies between 4.0 and 6.7 (2.8 on day August 08), using data from Fig. 4.

Figure 6 shows a scatterplot between IO and BrO column amounts from the individual satellite observations. Data from four days August 09 to 12 is included in the comparison. As in the correlation analysis mentioned in Sec.3.4, for each day those measurements are used that fall into a rectangular area enclosing the volcanic plume. The slope for all data of IO vs. BrO

25 columns is 0.09 with a correlation coefficient of 0.74. This observation is consistent with findings by Aiuppa et al. (2009) who estimate a one order of magnitude difference between the volcanic abundances of the two halogen species. In addition, Pyle and Mather (2009) estimate the annual fluxes of volcanic HBr and HI to be on the order of 5-15 Gg/year for HBr and 0.5-2 Gg/year for HI, respectively. The uncertainties given by the latter study are rather large, but the results agree on the difference of one order of magnitude between the two halogens.

30 The interesting point is that the seawater abundance yields a ratio of Br/I of 15,000, i.e. a four orders of magnitude difference between I and Br. This implies that the iodine vs. bromine ratio in the volcanic plume is enhanced by about three orders of magnitude judging from the IO and BrO observations. While other studies have shown that the Cl vs. Br ratio for volcanic condensates is in agreement with the seawater ratio of around 650 (Gerlach, 2004; Aiuppa et al., 2005), the ratio of Cl vs. I is

about two orders of magnitude lower than in seawater (Honda et al., 1966; Honda, 1970; Snyder and Fehn, 2002; Aiuppa et al., 2005). Consequently, an enhancement of iodine species takes place in the processes which determine the release of halogens from volcanic activity.

Explanations for the observed enhancement of iodine relative to seawater are connected to the magma composition of the

5 specific volcano. As Kasatochi is an oceanic arc volcano, marine sediments which are carried into the Earth mantle at the subduction zone, directly influence the composition of the volcanic material. Marine sediments in turn are enriched in iodine compounds from organic material (Muramatsu and Wedepohl, 1998). In addition, volcanic emissions are influenced by the composition of the melts and fluids in the volcanic chamber. Hydrothermal experiments have been used to analyse the compositions of hydrous fluids and silicate melts with respect to the different halogens (Bureau et al., 2000). It was found that the

10 partition coefficient between fluid and melt is clearly larger for iodine than for bromine and chlorine. The partitioning into the fluid phase is therefore stronger for iodine than for bromine which is again stronger as for chlorine. Consequently, volcanic emissions to the atmosphere are expected to be enhanced in iodine relative to the other halogens.

The temporal evolution of the observed IO and BrO amounts in the plume is of interest. The observations on the first day after the eruption, however, may be influenced by dust and clouds accompanying the eruption especially close to the volcano (Theys

15 et al., 2009). Consequently, trace gas amounts could be larger than quantified by the spectroscopic observations. Comparison of the temporal behaviour of IO and BrO shows that their evolution is similar with maximum integral amounts occurring one to three days after the eruption. BrO reaches its highest values (around 5×10^{29} molecules) earlier than IO. Different chemical pathways and time constants for IO and BrO production and destruction will influence the temporal variation in the ratios. However, the temporal changes between August 09 and 12 are close to the limit of being significant. Considering only the 1σ

20 standard deviation of IO on the order of 2.5×10^{12} molec/cm^2, the uncertainty on the integrated IO molecule number within the volcanic plume lies between 0.8 and 1.2 $\times 10^{28}$, using the plume areas from August 09 and 11, respectively. As a result, details in the temporal evolution need to be interpreted with care.

For an estimate of the impact of volcanic iodine on atmospheric chemistry, the volume mixing ratio (vmr) is a more relevant quantity than the column amount. For a rough estimate, the vertical plume extent derived by Theys et al. (2009) is used. They

25 determine the major part of the plume to reside between 8 and 12 km altitude. The retrieved number of IO molecules of around 5×10^{28} molecules from days August 10 and 11 is used as lower limit of the emitted iodine amount. The lateral plume extent on these days lies around 5×10^5 km^2. Spreading the observed IO homogeneously within the 4 km thick layer and over the entire plume extent, the average vmr would be around 3 pptv at 10 km altitude using US standard atmosphere pressure and temperature values. Certainly, local vmr values will exceed this average number due to an inhomogeneous distribution within

30 the plume. An iodine abundance of 3 pptv strongly impacts, e.g., on the ozone levels (Bösch et al., 2003; Saiz-Lopez et al., 2015a) and constitutes a large perturbation of stratospheric iodine, which is measured and estimated to be on the sub-pptv level. Iodine from volcanic eruptions has several possible implications for atmospheric composition. The Kasatochi plume altitude reaches into the lower stratosphere. Consequently, the satellite observations of large amounts of iodine after the Kasatochi eruption indicate, that volcanic eruptions may lead to a substantial input of iodine to the stratosphere as well as the upper

35 troposphere lower stratosphere (UTLS) region, depending on the eruption altitude and plume rise.

Due to the larger chain length for the removal of O_3 by BrO_x and IO_x than by ClO_x, loss of O_3 in the stratosphere can be significantly impacted by the BrO and IO in addition to ClO released from volcanic eruptions. In this case the lower stratosphere will be most affected. This could impact on ozone hole chemistry when volcanic eruptions enter the polar vortices, an issue recently raised by Solomon et al. (2016).

5 Background iodine amounts between 0.1 and 0.4 pptv in the free troposphere as observed recently (Puentedura et al., 2012; Dix et al., 2013) are possibly also influenced by volcanic activity. Following a volcanic eruption, the iodine amount will directly influence the local and regional chemistry by reducing the ozone levels. The impact of the ability of volcanic IO to form aerosol condensation nuclei requires further study. In addition, volcanic plumes may be subject to long-range transport and therefore lead to effects also at larger distances.

10 The Kasatochi eruption was in some respect special as it was a major eruption, the plume altitude was relatively large and also bromine amounts were larger than for other investigated volcanic plumes (Hörmann et al., 2013). IO has not yet been detected for any other eruptions investigated, at least not at the Kasatochi levels. Scaling with the observed bromine amounts, iodine levels for the other eruptions could just be below or around the detection limit of current space based instruments. Future satellite instruments with finer spatial resolution and improved signal-to-noise ratio may allow the observation and detailed

15 investigation of iodine species in volcanic plumes more frequently.

It is interesting to speculate on the amount of halogens emitted to the atmosphere from past major eruptions which have severely impacted on atmospheric composition prior to halogen observations from space. For the Pinatubo eruption in 1991, for example, a total mass of about 20 Tg of SO_2 was emitted. The eruption injected gases and aerosols up to 25-30 km altitude, i.e. around the maximum stratospheric ozone mixing ratio. In relative terms, the IO vmr will be increased at these high alti-

20 tudes due to much lower air density as compared to the Kasatochi estimates. Assuming a similar magma composition as that for Kasatochi, i.e. similar halogen to sulphur ratios, an amount of around 100 t of IO as well as 1 kt of BrO could have been emitted into the stratosphere from Pinatubo with corresponding impact on stratospheric chemistry over extended horizontal distances and periods. A detailed assessment again requires better knowledge and studies of the loss of iodine and bromine in the stratospheric aerosol.

25 **5 Summary and Conclusions**

For several days following the major eruption of Kasatochi volcano in August 2008, iodine monoxide was observed by satellite measurements in the emitted volcanic plume. This is the first experimental evidence of IO from a volcanic eruption. The satellite sensors SCIAMACHY and GOME-2A both detect slant column amounts of IO above 4×10^{13} molec/cm^2 in the volcanic plume for several days following the Kasatochi eruption. Maximum vertical columns above 2×10^{13} molec/cm^2 are derived.

30 The presented observations also represent the first reported retrievals of IO from measurements of the GOME-2A instrument. In comparison to tropospheric IO observations in polar and mid-latitudinal regions, the observed column amounts are large, reducing the uncertainties and facilitating analysis of individual measurements. The IO data in the plume shows good fitting quality with fitting errors around 6% for SCIAMACHY and below 15% for GOME-2A retrievals.

Overall, the IO enhancements coincide in space with previously published BrO and SO_2 observations. While the plumes of IO, BrO and SO_2 are roughly found in the same area with similar shape, the maximum amounts of the individual species, however, do not always coincide. Differences between IO and BrO are smaller than those between the halogens and SO_2. The emission chronology as well as chemical conversions are presumably individual for the three compounds and could probably lead to the observed differences in spatial distributions.

Correlating all observations of IO and BrO between August 9 to 12 yields a slope of 0.09, i.e. IO amounts are about one order of magnitude smaller than those of BrO. This means a three order of magnitude difference with respect to the seawater ratio in agreement with previous filter measurements of volcanic samples at arc volcanos. For this relative enhancement of iodine two reasons play a role. Iodine shows a stronger preference than bromine to partition into volcanic fluids than volcanic melts in the volcanic chamber below the volcano. This relative partitioning between fluid and melt determines the gas phase composition from an eruption. In addition, iodine enriched marine sediments are carried into the Earth's mantle in the subduction zone and directly influence the composition of the magma.

An integration of the observed IO amount within the emission plume results in a large mass of around 10 t (4 to 12 t) of IO emitted from the volcano. Comparing these numbers to the results of BrO, the ratio for BrO to IO molecules lies between 6.7 and 10.0, while the ratio for the mass of BrO to IO lies between 4.0 and 6.7. Together with the knowledge that the Kasatochi BrO plume reached predominantly the altitude between 8 and 12 km, it can be concluded that a substantial input of iodine to the stratosphere, UTLS and free troposphere has taken place following the Kasatochi eruption. If the IO amount is homogeneously spread over the plume area and within the main 4 km thick vertical layer, a vmr of 3 pptv at an altitude of 10 km results. The local vmr can be much higher due to inhomogeneous distribution in the volcanic plume. An iodine vmr of around 3 pptv has substantial impact on the atmospheric composition, e.g., through reducing the ozone levels.

The investigation of past and future volcanic eruptions with respect to their IO content and impact on tropospheric and stratospheric chemistry is subject to further work and will be facilitated in the future by improved satellite instrumentation.

Acknowledgements. SCIAMACHY lv1 data have been provided by ESA (European Space Agency) and DLR (Deutsches Zentrum für Luft- und Raumfahrt), GOME-2A lv1 data have been provided by EUMETSAT. Financial support through the University of Bremen Institutional Strategy Measure M8 in the framework of the DFG Excellence Initiative is gratefully acknowledged for AS. This study is in part a contribution to the DFG SFB TR 172.

References

Aiuppa, A., Federico, C., Franco, A., Giudice, G., Gurrieri, S., Inguaggiato, S., Liuzzo, M., McGonigle, A. J. S., and Valenza, M.: Emission of bromine and iodine from Mount Etna volcano, Geochemistry Geophysics Geosystems, 6, doi:10.1029/2005GC000965, 2005.

Aiuppa, A., Baker, D., and Webster, J.: Halogens in volcanic systems, Chemical Geology, 263, 1–18, doi:http://dx.doi.org/10.1016/j.chemgeo.2008.10.005, 2009.

Alicke, B., Hebestreit, K., Stutz, J., and Platt, U.: Iodine oxide in the marine boundary layer, Nature, 397, 572–573, 1999.

Begoin, M., Richter, A., Weber, M., Kaleschke, L., Tian-Kunze, X., Stohl, A., N., T., and Burrows, J. P.: Satellite observations of long range transport of a large BrO cloud in the Arctic, Atmospheric Chemistry and Physics, 10, 6515–6526, 2010.

Bobrowski, N. and Platt, U.: SO2/BrO ratios studied in five volcanic plumes, Journal of Volcanology and Geothermal Research, 166, 147 – 160, doi:http://dx.doi.org/10.1016/j.jvolgeores.2007.07.003, 2007.

Bobrowski, N., Hönninger, G., Galle, B., and Platt, U.: Detection of bromine monoxide in a volcanic plume, Nature, 423, 273–276, 2003.

Bobrowski, N., Hönninger, G., Lohberger, F., and U., P.: IDOAS: A new monitoring technique to study the 2D distribution of volcanic gas emissions, Journal of Volcanology and Geothermal Research, 150, 329–338, doi:10.1016/j.jvolgeores.2005.05.004, 2006.

Bobrowski, N., von Glasow, R., Aiuppa, A., Inguaggiato, S., Louban, I., Ibrahim, O. W., and Platt, U.: Reactive halogen chemistry in volcanic plumes, J. Geophys. Res. Atmos., 112, 2007.

Bogumil, K., Orphal, J., Homann, T., Voigt, S., Spietz, P., Fleischmann, O. C., Vogel, A., Hartmann, M., Bovensmann, H., Frerik, J., and Burrows, J. P.: Measurements of Molecular Absorption Spectra with the SCIAMACHY Pre-Flight Model: Instrument Characterization and Reference Data for Atmospheric Remote-Sensing in the 230-2380 nm Region, J. Photochem. Photobiol. A, 157, 167–184, 2003.

Bösch, H., Camy-Peyret, C., Chipperfield, M. P., Fitzenberger, R., Harder, H., Platt, U., and Pfeilsticker, K.: Upper limits of stratospheric IO and OIO inferred from center-to-limb-darkening-corrected balloon-borne solar occultation visible spectra: Implications for total gaseous iodine and stratospheric ozone, J. Geophys. Res., 108, doi:10.1029/2002JD003078, 2003.

Bovensmann, H., Burrows, J. P., Buchwitz, M., Frerick, J., Noël, S., Rozanov, V. V., Chance, K. V., and Goede, A. P. H.: SCIAMACHY: Mission Objectives and Measurement Modes, J. Atmos. Sci., 56, 127–150, 1999.

Bureau, H., Keppler, H., and Métrich, N.: Volcanic degassing of bromine and iodine: experimental fluid/melt partitioning data and applications to stratospheric chemistry, Earth and Planetary Science Letters, 183, 51–60, 2000.

Burkholder, J. B., Curtius, J., Ravishankara, A. R., and Lovejoy, E. R.: Laboratory studies of the homogeneous nucleation of iodine oxides, Atmospheric Chemistry and Physics, 4, 19–34, 2004.

Burrows, J. P., Hölzle, E., Goede, A. P. H., Visser, H., , and Fricke, W.: SCIAMACHY - Scanning Imaging Absorption Spectrometer for Atmospheric Chartography, Acta Astronautica, 35, 445–451, 1995.

Carpenter, L. J.: Iodine in the Marine Boundary Layer, Chem. Rev., 103, 4953–4962, 2003.

Carpenter, L. J., MacDonald, S. M., Shaw, M. D., Kumar, R., Saunders, R. W., Parthipan, R., Julie, W., and Plane, J. M. C.: Atmospheric iodine levels influenced by sea surface emissions of inorganic iodine, Nature Geoscience, 6, 108–111, doi:10.1038/ngeo1687, 2013.

Chameides, W. L. and Davis, D. D.: Iodine: its possible role in tropospheric chemistry, J. Geophys. Res., 85, 7383–7398, 1980.

Chehade, W., Guer, B., Spietz, P., Gorshelev, V., Serdyuchenko, A., Burrows, J. P., and Weber, M.: Temperature dependent ozone absorption cross section spectra measured with the GOME-2 FM3 spectrometer and first application in satellite retrievals, Atmospheric Measurement Techniques, 6, 1623–1632, doi:10.5194/amt-6-1623-2013, 2013.

Dix, B., Baidar, S., Bresch, J. F., Hall, S. R., Schmidt, K. S., Wang, S., and Volkamer, R.: Detection of iodine monoxide in the tropical free troposphere, PNAS, 110, 2035–2040, doi:10.1073/pnas.1212386110, www.pnas.org/cgi/doi/10.1073/pnas.1212386110, 2013.

Garland, J. A. and Curtis, H.: Emission of Iodine From the Sea Surface in the Presence of Ozone, JOURNAL OF GEOPHYSICAL RESEARCH, 86, 3183–3186, 1981.

5 General, S., Bobrowski, N., Pöhler, D., Weber, K., Fischer, C., and Platt, U.: Airborne I-DOAS measurements at Mt. Etna: BrO and OClO evolution in the plume, Journal of Volcanology and Geothermal Research, 300, 175–186, doi:http://dx.doi.org/10.1016/j.jvolgeores.2014.05.012, 2015.

Gerlach, T. M.: Volcanic sources of tropospheric ozone-depleting trace gases, Geochemistry, Geophysics, Geosystems, 5, doi:10.1029/2004GC000747, 2004.

10 Gómez Martín, J. C., Spietz, P., and Burrows, J. P.: Kinetic and Mechanistic Studies of the I_2/O_3 Photochemistry, J. Phys. Chem. A., 111, doi:10.1021/jp061186c, 2007.

Gottwald, Manfred und Bovensmann, H., ed.: SCIAMACHY Exploring the Changing Earth's Atmosphere, Earth and Environmental Science. Springer Dordrecht Heidelberg London New York, 2011.

Greenblatt, G. D., Orlando, J. J., Burkholder, J. B., and Ravishankara, A. R.: Absorption Measurements of Oxygen Between 330 and 1140
15 nm, J. Geophys. Res., 95(D11), 18 577–18 582, 1990.

Honda, F.: Geochemical study of iodine in volcanic gases. II. Behavior of iodine in volcanic gases., Geochemical Journal, 3, 201 – 211, 1970.

Honda, F., Mizutani, Y., Sugiura, T., and Oana, S.: A Geochemical Study of Iodine in Volcanic Gases, Bulletin of the Chemical Society of Japan, 39, 2690 – 2695, 1966.

Hörmann, C., Sihler, H., Bobrowski, N., Beirle, S., Penning de Vries, M., Platt, U., and Wagner, T.: Systematic investigation of bromine
20 monoxide in volcanic plumes from space by using the GOME-2 instrument, Atmospheric Chemistry and Physics, 13, 4749–4781, doi:10.5194/acp-13-4749-2013, http://www.atmos-chem-phys.net/13/4749/2013/, 2013.

Kern, C., Sihler, H., Vogel, L., Rivera, C., Herrera, M., and Platt, U.: Halogen oxide measurements at Masaya Volcano, Nicaragua using active long path differential optical absorption spectroscopy, Bulletin of Volcanology, 71, 659–670, doi:10.1007/s00445-008-0252-8, 2009.

Lee, C., Kim, Y. J., Tanimoto, H., Bobrowski, N., Platt, U., Mori, T., Yamamoto, K., and Hong, C. S.: High ClO and ozone depletion observed
25 in the plume of Sakurajima volcano, Japan, Geophysical Research Letters, 32, doi:10.1029/2005GL023785, l21809, 2005.

Muramatsu, Y. and Wedepohl, K. H.: The distribution of iodine in the earth's crust, Chemical Geology, 147, 201–216, doi:http://dx.doi.org/10.1016/S0009-2541(98)00013-8, 1998.

Newhall, C. G. and Self, S.: The volcanic explosivity index (VEI) an estimate of explosive magnitude for historical volcanism, Journal of Geophysical Research: Oceans, 87, 1231–1238, doi:10.1029/JC087iC02p01231, 1982.

30 O'Dowd, C. D. and Hoffmann, T.: Coastal New Particle Formation: A Review of the Current State-Of-The-Art, Environ. Chem., 2, doi:10.1071/EN05077, 2005.

Platt, U. and Stutz, J.: Differential Optical Absorption Spectroscopy - Principles and Applications, Springer-Verlag, 2008.

Puentedura, O., Gil, M., Saiz-Lopez, A., Hay, T., Navarro-Comas, M., Gómez-Pelaez, A., Cuevas, E., Iglesias, J., and Gomez, L.: Iodine monoxide in the north subtropical free troposphere, Atmospheric Chemistry and Physics, 12, 4909–4921, doi:10.5194/acp-12-4909-2012,
35 http://www.atmos-chem-phys.net/12/4909/2012/, 2012.

Pyle, D. and Mather, T.: Halogens in igneous processes and their fluxes to the atmosphere and oceans from volcanic activity: a review, Chemical Geology, 263, 110–121, doi:doi:10.1016/j.chemgeo.2008.11.013, 2009.

Richter, A.: GOME-2 volcanic SO$_2$ algorithm theoretical basis document, Support to Aviation for Volcanic Ash Avoidance, Norw. Inst. for Air Res., Kjeller, Norway, available at http://savaa.nilu.no/ PublicArchive/tabid/3207/Default.aspx, 2009.

Rozanov, V. V., Rozanov, A. V., Kokhanovsky, A. A., and Burrows, J. P.: Radiative transfer through terrestrial atmosphere and ocean: Software package SCIATRAN, Journal of Quantitative Spectroscopy and Radiative Transfer, 133, 13–71, doi:10.1016/j.jqsrt.2013.07.004, 2014.

Saiz-Lopez, A., Chance, K., Liu, X., Kurosu, T. P., and Sander, S. P.: First observations of iodine oxide from space, Geophys. Res. Lett., 34, doi:doi:10.1029/2007GL030111, 2007.

Saiz-Lopez, A., Plane, J. M. C., Baker, A. R., Carpenter, L. J., von Glasow, R., Gómez-Martín, J. C., McFiggans, G., and Saunders, R. W.: Atmospheric Chemistry of Iodine, Chemical Reviews, 112, 1773–1804, doi:10.1021/cr200029u, 2012.

Saiz-Lopez, A., Baidar, S., Cuevas, C. A., Koenig, T. K., Fernandez, R. P., Dix, B., Kinnison, D. E., Lamarque, J.-F., Rodriguez-Lloveras, X., Campos, T. L., and Volkamer, R.: Injection of iodine to the stratosphere, Geophysical Research Letters, 42, 6852–6859, doi:10.1002/2015GL064796, 2015a.

Saiz-Lopez, A., Blaszczak-Boxe, C. S., and Carpenter, L. J.: A mechanism for biologically induced iodine emissions from sea ice, Atmospheric Chemistry and Physics, 15, 9731–9746, doi:10.5194/acp-15-9731-2015, 2015b.

Saunders, R., Kumar, R., Gomez-Martin, J., Mahajan, A., Murray, B., and Plane, J.: Studies of the formation and growth of aerosol from molecular iodine precursor, Z. Phys. Chem., 224, 1095–1117, doi:10.1524/zpch.2010.6143, 2010.

Schall, C., Laturnus, F., and Heumann, K. G.: Biogenic volatile organoiodine and organobromine compounds released from polar macroalgae, Chemosphere, 28, 1315–1324, 1994.

Schönhardt, A., Richter, A., Wittrock, F., Kirk, H., Oetjen, H., Roscoe, H. K., and Burrows, J. P.: Observations of iodine monoxide columns from satellite, Atmos. Chem. Phys., 8, 637–653, 2008.

Schönhardt, A., Begoin, M., Richter, A., Wittrock, F., Kaleschke, L., Gómez Martín, J. C., and Burrows, J. P.: Simultaneous satellite observations of IO and BrO over Antarctica, Atmospheric Chemistry and Physics, 12, 6565–6580, doi:10.5194/acp-12-6565-2012, http://www.atmos-chem-phys.net/12/6565/2012/, 2012.

Snyder, G. T. and Fehn, U.: Origin of iodine in volcanic fluids: ^{129}I results from the Central American Volcanic Arc, Geochimica et Cosmochimica Acta, 66, 3827–3838, 2002.

Solomon, S., Garcia, R. R., and Ravishankara, A. R.: On the role of iodine in ozone depletion, J. Geophys. Res., 99, 20 491–20 499, 1994.

Solomon, S., Ivy, D. J., Kinnison, D., Mills, M. J., Neely, R. R., and Schmidt, A.: Emergence of healing in the Antarctic ozone layer, Science, doi:10.1126/science.aae0061, http://science.sciencemag.org/content/early/2016/06/30/science.aae0061, 2016.

Surl, L., Donohoue, D., Aiuppa, A., Bobrowski, N., and von Glasow, R.: Quantification of the depletion of ozone in the plume of Mount Etna, Atmospheric Chemistry and Physics, 15, 2613–2628, doi:10.5194/acp-15-2613-2015, 2015.

Theys, N., Van Roozendael, M., Dils, B., Hendrick, F., Hao, N., and De Mazière, M.: First satellite detection of volcanic bromine monoxide emission after the Kasatochi eruption, Geophysical Research Letters, 36, doi:10.1029/2008GL036552, 2009.

Theys, N., De Smedt, I., Van Roozendael, M., Froidevaux, L., Clarisse, L., and Hendrick, F.: First satellite detection of volcanic OClO after the eruption of Puyehue-Cordón Caulle, Geophysical Research Letters, 41, 667–672, doi:10.1002/2013GL058416, http://dx.doi.org/10.1002/2013GL058416, 2014.

Vogt, R., Sander, R., von Glasow, R., and Crutzen, P. J.: Iodine Chemistry and its role in Halogen Activation and Ozone Loss In the Marine Boundary Layer: A Model Study., J. Atmos. Chem., 32, 375–395, 1999.

von Glasow, R., Bobrowski, N., and Kern, C.: The effects of volcanic eruptions on atmospheric chemistry, Chemical Geology, 263, 131–142, doi:http://dx.doi.org/10.1016/j.chemgeo.2008.08.020, 2009.
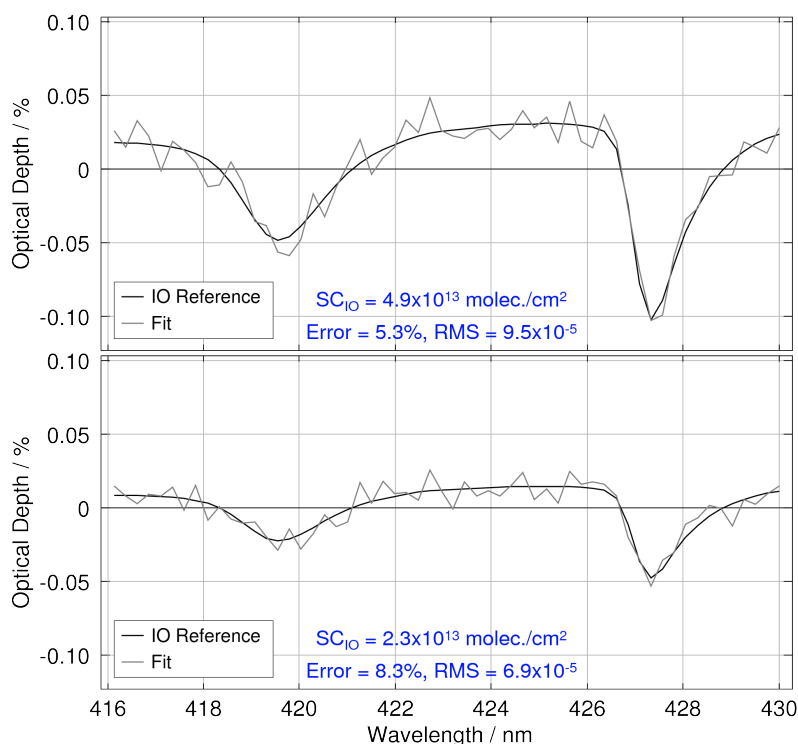
Figure 1. Example fitting results from SCIAMACHY on day August 11, 2008, with two different IO slant column amounts recorded at 55.34°N, 220.21°E (top) and 54.90°N, 215.92°E (bottom). The fit (grey) shows the measurement optical depth after all other features except for the IO absorption (black) have been subtracted. The optical depth RMS values are 9.5 and 6.9 $\times 10^{-5}$, respectively.

Vountas, M., Rozanov, V. V., and Burrows, J. P.: Ring effect: Impact of rotational Raman scattering on radiative transfer in Earth's atmosphere, J. Quant. Spectrosc. Radiat. Transfer, 60, 943–961, 1998.

Waythomas, C. F., Scott, W. E., Prejean, S. G., Schneider, D. J., Izbekov, P., and Nye, C. J.: The 7-8 August 2008 eruption of Kasatochi Volcano, central Aleutian Islands, Alaska, Journal of Geophysical Research: Solid Earth, 115, doi:10.1029/2010JB007437, 2010.

5 Witt, M. L. I., Mather, T. A., Pyle, D. M., Aiuppa, A., Bagnato, E., and Tsanev, V. I.: Mercury and halogen emissions from Masaya and Telica volcanoes, Nicaragua, Journal of Geophysical Research: Solid Earth, 113, doi:10.1029/2007JB005401, 2008.

World Meteorological Organization: Scientific Assessment of Ozone Depletion: 2014, World Meteorological Organization (WMO), Global Ozone Research and Monitoring Project-Report No. 55, World Meteorological Organization, 416 pp., 2014.
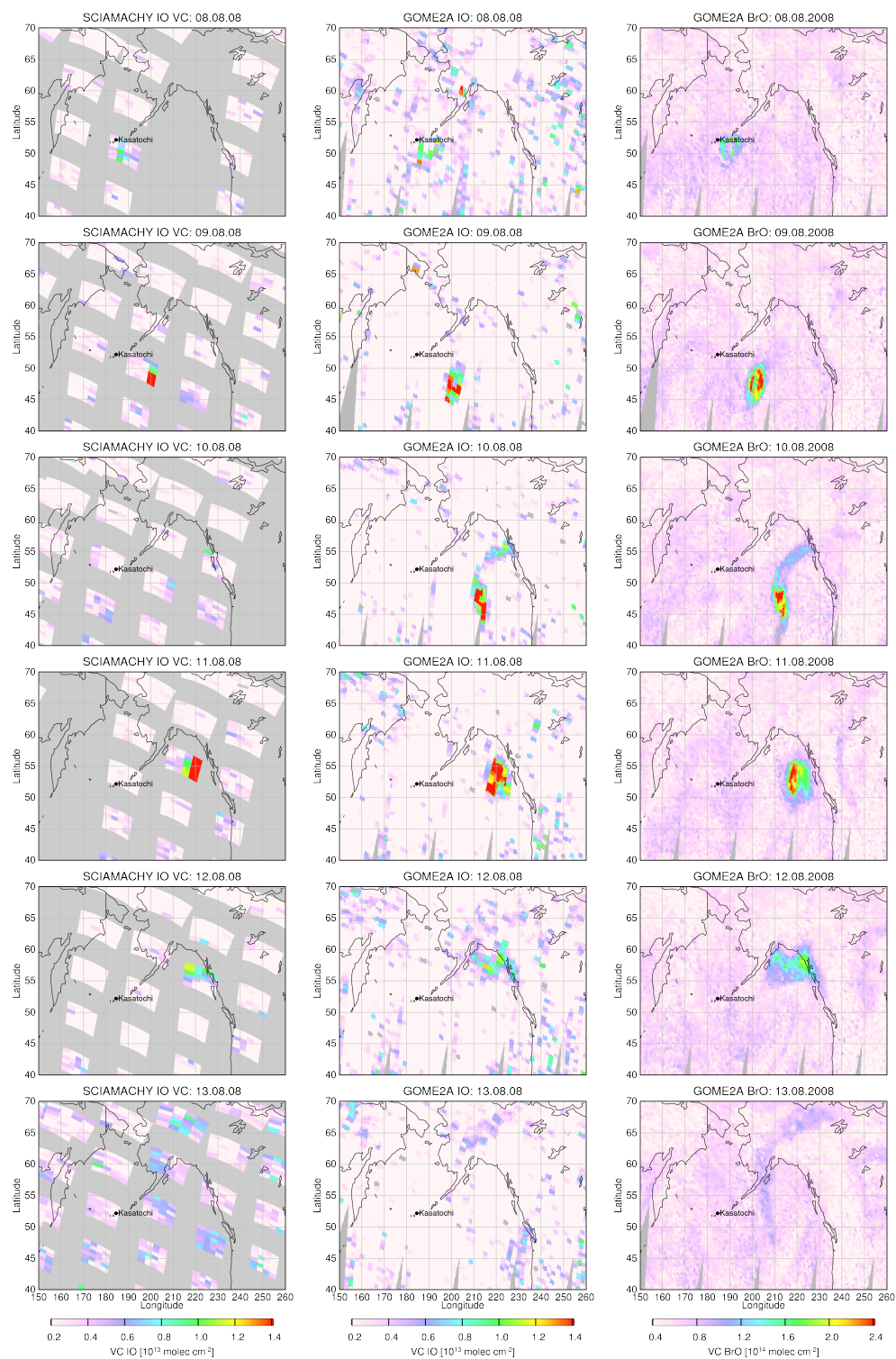
Figure 2. Retrievals of IO from SCIAMACHY (left) and GOME-2A (middle) together with observations of BrO from GOME-2A (right) for 6 days following the eruption of Kasatochi volcano on August 08, 2008. Regions without data coverage are shaded in grey.
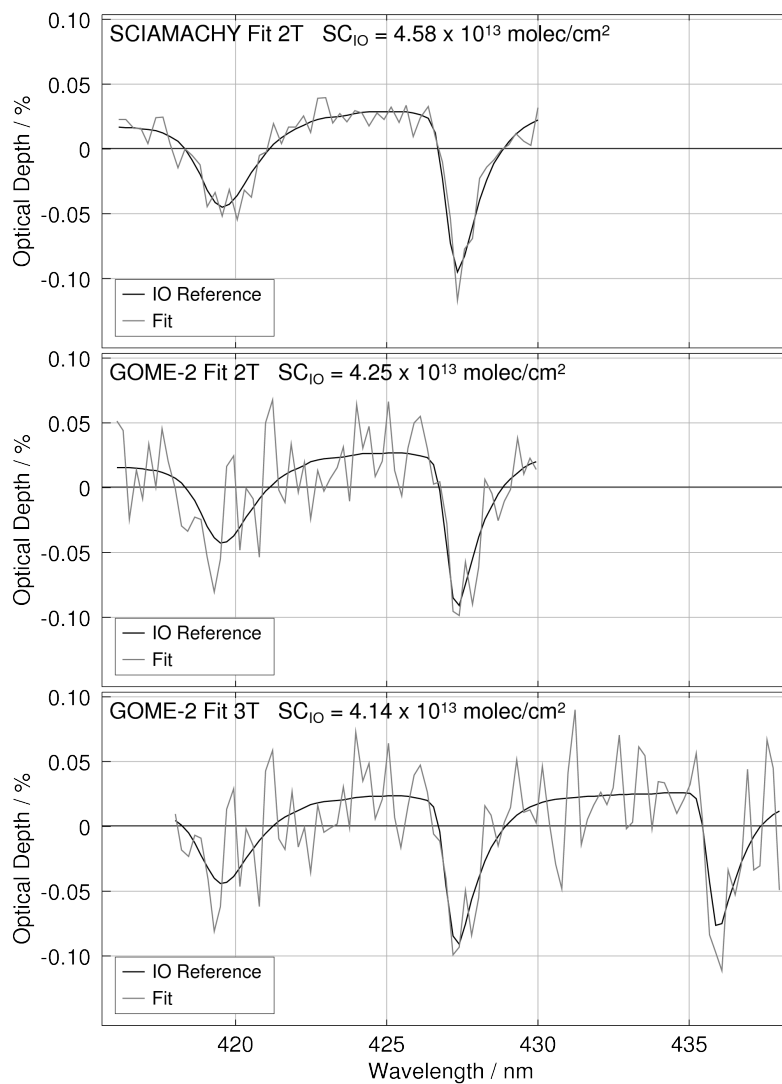
Figure 3. Spectral fitting results from day August 11, 2008, for a collocation between SCIAMACHY (top) and GOME-2A around 55°N and 220°E. For GOME-2A, the results from two different fitting windows are shown, using the SCIAMACHY standard IO fitting window (center) and using a larger spectral window covering three spectral bands of IO (bottom).
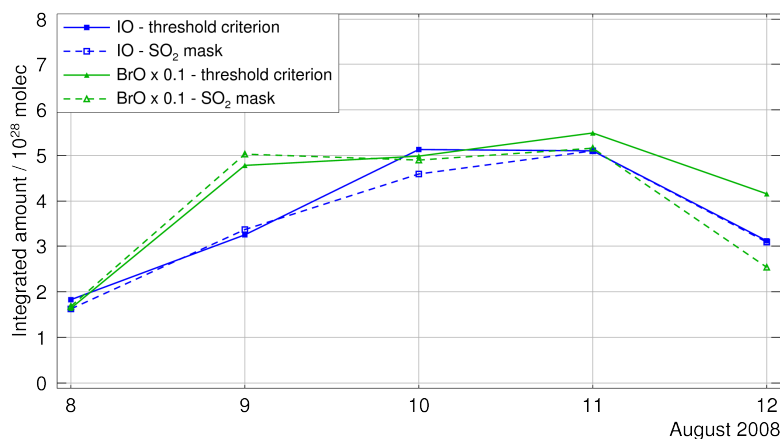
Figure 4. Time series of integrated IO (blue) and BrO (green) amounts. BrO data is scaled by a factor of 0.1. For both trace gases, two methods for the plume definition are applied, the threshold criterion and the SO$_2$ mask.
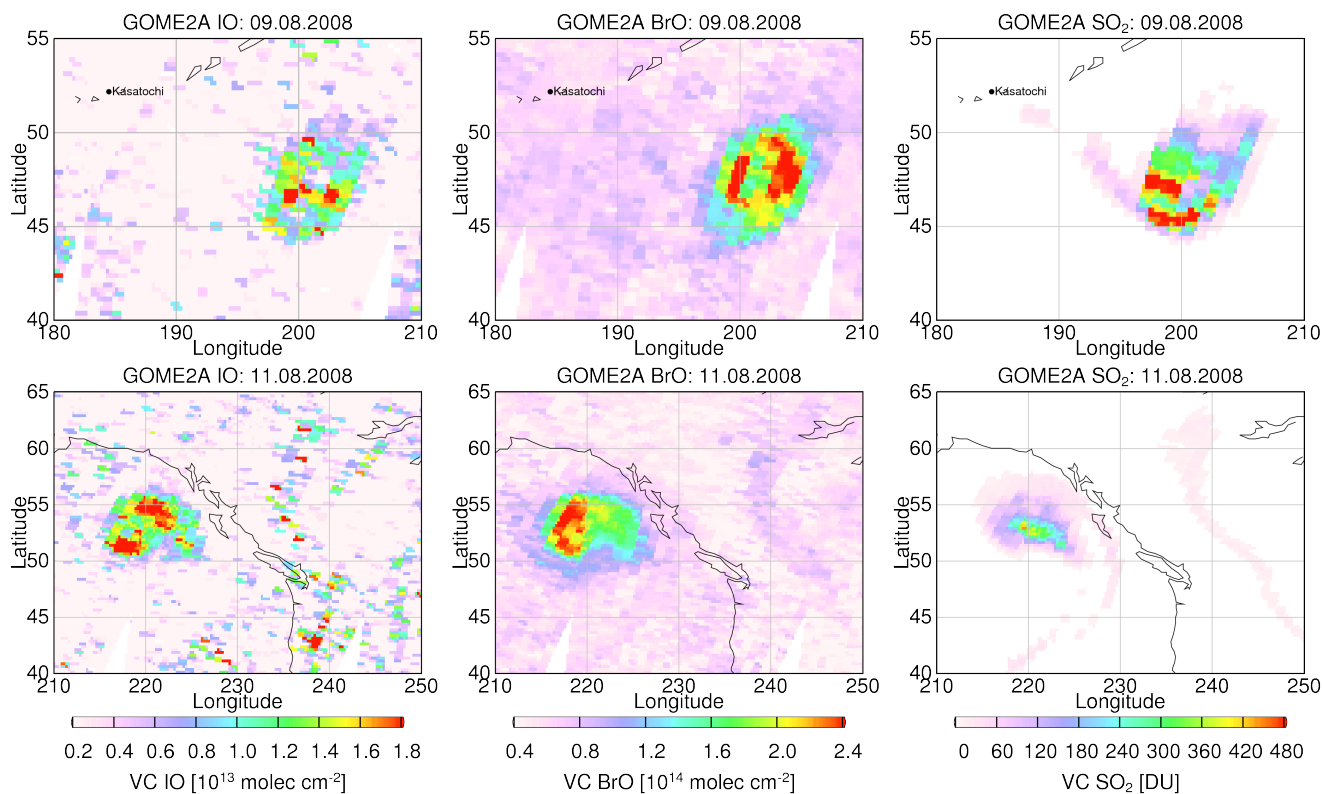
Figure 5. Close-up of the volcanic plumes of IO (left), BrO (center) and SO$_2$ (right) on the days August 09 (top) and August 11 (bottom). While the plume extent and shape are similar, differences in the spatial distribution patterns are visible.
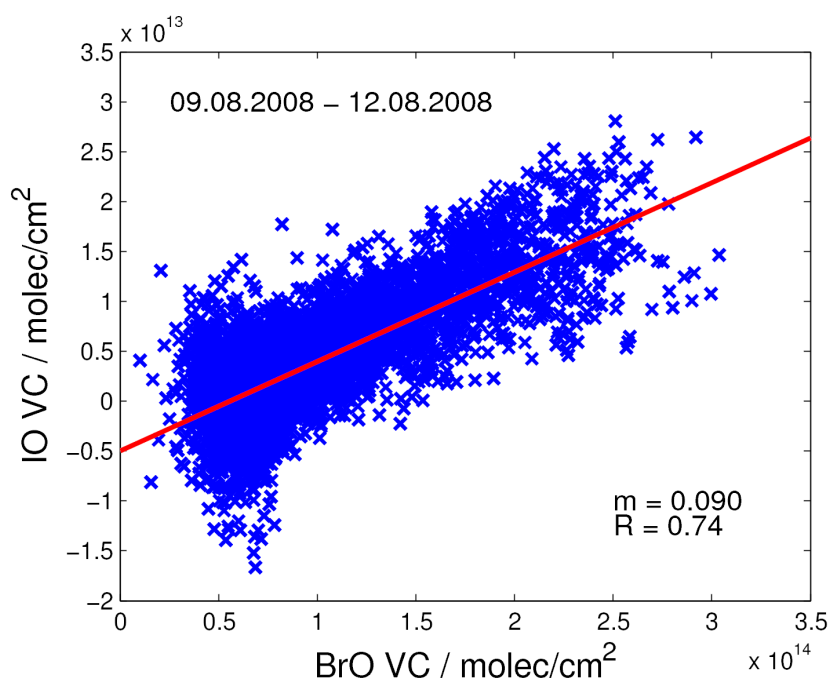
Figure 6. Scatterplot of IO vs. BrO column amounts. Data from the four days August 09 to 12, 2008, is included.